Mechanical Properties and Microstructures of SiC Fiber-reinforced Metal Matrix Composites Made Using Ultrasonic Consolidation

Y. YANG
Department of Mechanical and Aerospace Engineering, Utah State University, Logan, UT 84322-4130, USA

B. E. STUCKER*
Department of Industrial Engineering, University of Louisville, Louisville, KY 40292, USA

G. D. JANAKI RAM
Department of Metallurgical and Materials Engineering, Indian Institute of Technology Madras, Chennai 600036, India

ABSTRACT: Ultrasonic consolidation was used for making SiC fiber-reinforced Al 3003 matrix composites. Peel tests, tensile tests, and bend tests were carried out on the composite specimens as well as on ultrasonically consolidated Al 3003 specimens containing no SiC fibers. The objective of this study was to examine whether the ultrasonically embedded SiC fibers serve as effective reinforcements or not. Incorporation of SiC fibers resulted in a considerable improvement in peel strength and tensile strength of ultrasonically consolidated parts. However, bend tests revealed some deterioration in the shear strength of the parts due to the presence of fibers. The results of mechanical testing are discussed based on microstructural and fractographic studies.

KEY WORDS: ultrasonic consolidation, metal matrix composites, microstructures, mechanical properties, fracture features.

INTRODUCTION

ULTRASONIC CONSOLIDATION (UC) is a novel additive manufacturing process implementing ultrasonic metal welding and computer numerical controlled (CNC) milling techniques for fabrication of complex three-dimensional structures from metal foils [1].

*Author to whom correspondence should be addressed. E-mail: brent.stucker@louisville.edu
Figure 6 appears in color online: http://jcm.sagepub.com

0021-9983/10/26 3179–16 $10.00/0 DOI: 10.1177/0021998310371528

Previous investigations have demonstrated the unique capabilities of this process in fabricating multifunctional structures with high dimensional accuracy and desirable surface finish, including objects with complex internal features, objects made up of multiple materials, and objects integrated with wiring, electronics, and fiber optics [2–4].

UC is conducted on a machine tool, which was commercially introduced by Solidica Inc., in the year 2000. The Solidica Formation^{TM} UC machine incorporates an ultrasonic metal welding head, a 3-axes milling head, a foil feeding apparatus, and a software program to automatically generate tool paths for metal foil deposition and machining. In UC, a three-dimensional CAD model of the part to be built is initially generated. A computer software program slices the CAD model into a number of horizontal layers. These layers are systematically deposited one over another to make the part. Typically, the layer thickness is same as the thickness of the metal foil used, but in certain instances it is advantageous to mill the layer to a different thickness after each layer is deposited [5]. The width of the foil is typically 25 mm.

Figure 1 illustrates the basic principle of UC. In this process, a rotating sonotrode travels along the length direction of a metal foil placed over a substrate. The foil is held closely in contact with the substrate by applying a normal force via the rotating sonotrode. The sonotrode oscillates transversely to the direction of travel at a frequency of 20 kHz and at a user-set oscillation amplitude, while traveling over the metal foil. The combination of normal and oscillating shear forces results in dynamic interfacial stresses at the foil–substrate interface [1,6]. The stresses produce elastic–plastic deformation of surface asperities, which breaks up the surface oxide layer, producing metallurgical bonding across the clean metal surfaces. After depositing a strip of foil, another foil is deposited adjacent to it if necessary. This operation repeats until a complete layer is deposited. After depositing a certain number of layers (called a level), a computer controlled milling head shapes the layer(s) to the desired geometry. Four layers per level is the default setting for machining, that is, a milling operation occurs after depositing four layers of metal foils. Once the level is shaped to its contour, machining chips are blown away using compressed air and foil deposition starts for the next layer.

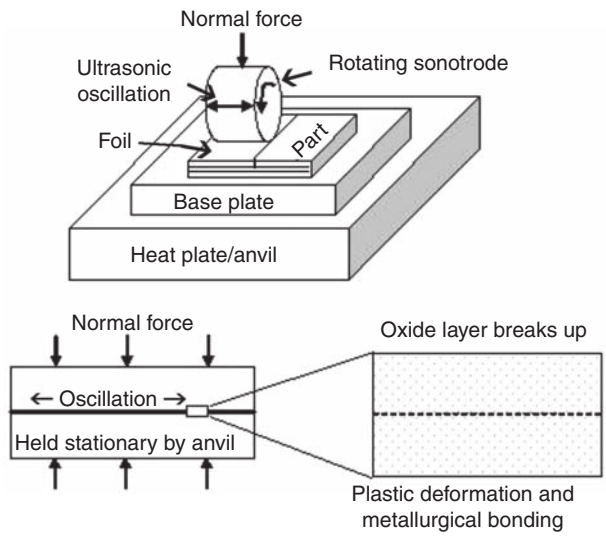

Figure 1. *Schematic of the UC process.*

Researchers have successfully embedded SiC fibers in Al matrices using UC, demonstrating the suitability of this process for manufacturing fiber-reinforced metal matrix composite (MMC) parts [7–9]. The available information in this regard primarily deals with optimization of UC process parameters for good fiber embedment [8,9]. Some information is available on fiber–matrix interface microstructures, which suggests that fibers are mechanically entrapped in metal matrices during UC [10,11]. However, practically no published data are available on the mechanical properties of UC-produced MMC parts. Thus, whether UC-fabricated MMC parts possess adequate mechanical properties or not is still a question that needs to be addressed. In view of the above, an attempt is made in this study to investigate the mechanical properties of UC-fabricated MMC specimens using peel tests, tensile tests, and three-point bend tests.

EXPERIMENTAL PROCEDURE

The materials used in this investigation were: (1) Al alloy 3003 foils in H18 temper (nominal composition by wt%: Al–1.2Mn–0.12Cu; 150 μm thick and 25 mm wide) and (2) SiC fibers (100 μm in diameter). The SiC fibers contained a 10 μm diameter tungsten core and a 1 μm thick carbon coating on the outer surface of the fiber. Al 3003 specimens were fabricated without and with embedded SiC fibers (hereafter referred as Type I and Type II specimens, respectively) in identical geometries for each of the three mechanical tests using a Formation™ UC machine equipped with a sonotrode of 140 mm in diameter.

Fabrication of Peel Test Specimens

Type I specimens for peel tests were fabricated using the following procedure (Figure 2). Initially, a single Al 3003 foil was fully consolidated to the substrate and machined to 125 mm in length. Next, another Al 3003 foil was deposited on the first foil, purposefully leaving a 25 mm offset (unwelded portion) at each end. Type II specimens were fabricated in a similar manner, but with three SiC fibers embedded between the first and the second Al foils.

The process parameters used for fabricating both types of specimens were: oscillation amplitude 13 μm; welding speed 32 mm/s; normal force 1450 N; and substrate temperature 150°C.

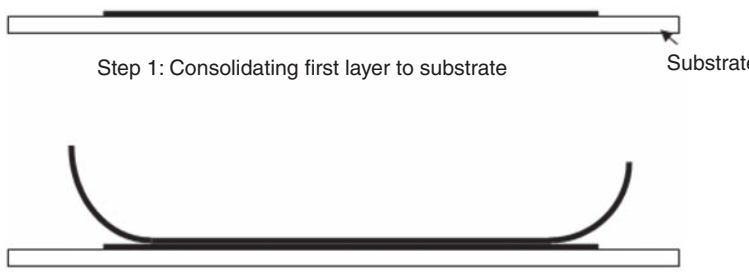

Figure 2. *Fabrication procedure for peel test specimens.*

UC parts made from 150 μm thick Al 3003 foils using the above-mentioned combination of process parameters typically show an average linear weld density (LWD) of 60% [5]. This combination of process parameters, rather than the optimum ones reported in a previous publication [5,9], was deliberately used to facilitate examination of possible enhancement of foil–foil bond strength due to presence of SiC fibers in specimens with otherwise low LWD. Three specimens of Type I and Type II each were prepared for peel tests.

Fabrication of Tensile Test Specimens

Tensile test specimens were designed and made according to ASTM D3552-96 standard (design F). Type I specimens were approximately 2.6 mm thick, which consisted of five levels (20 layers) of metal foils. The process parameters used for fabricating these specimens were: oscillation amplitude 16 μm; welding speed 32 mm/s; normal force 1750 N; and substrate temperature 150°C. UC specimens made from 150 μm thick Al 3003 foils using the aforesaid combination of process parameters typically show a high level of LWD [5].

Type II specimens had a geometry identical to Type I specimens and were made using the same combination of process parameters as Type I tensile specimens. In Type II specimens, the second, third, and forth levels contained SiC fibers (along the specimen length). Each of these three levels contained four SiC fibers (two fibers embedded between the first and the second layers and two more between the third and the fourth layers). No fibers were embedded in the first and fifth levels. Three specimens of Type I and Type II each were prepared for tensile tests.

Fabrication of Bend Test Specimens

Three-point bend test specimens ($14 \times 10 \times 2.6\,mm^3$) were made according to ASTM D2344-84, which contained five levels (20 layers) of metal foils. The process parameters used for fabricating the bend test specimens were identical to those used for the tensile test specimens. Once again, Type I and Type II specimens had a geometry identical. In Type II specimens, SiC fibers were embedded in the same manner as described for the tensile test specimens. Twenty Type I and twelve Type II specimens were prepared for the bend tests.

Mechanical Testing

In earlier studies, peel tests were used for evaluating the bond strength between ultrasonically consolidated metal foils [2,7]. In this study, peel tests were conducted to ascertain the influence of embedded SiC fibers on the bond strength between the ultrasonically consolidated metal foils. These tests were conducted on a standard tensile testing machine using a custom-designed fixture, as shown in Figure 3. During testing, the specimen to be tested was placed on the fixture, which was rigidly attached to the upper jaw of the tensile machine. The free end of the metal foil was placed between the rollers of the fixture and clamped to the lower jaw of the tensile machine. The upper jaw was set to move upward at a speed of 0.05 mm/s so that, during the upward motion of the fixture, the metal foil peels off the substrate. A load cell, which was attached to the lower jaw, was used to record the loading history. Totally, six tests were conducted for both Type I and Type II specimens.

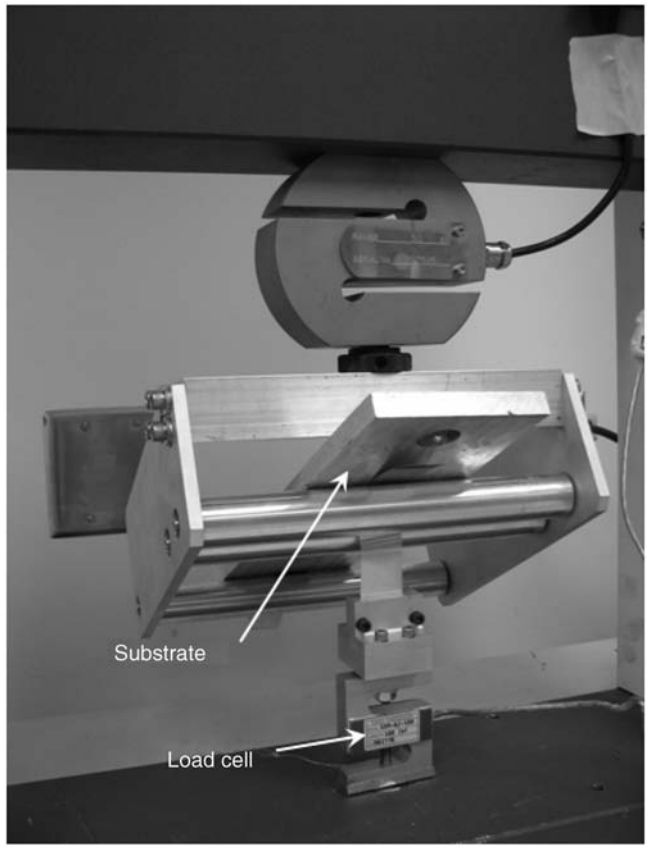

Figure 3. *Setup for peel tests.*

Tensile tests were conducted on a standard tensile machine using a crosshead travel speed of 0.017 mm/s (1 mm/min). Only the ultimate tensile strength (UTS) of the specimens was measured.

Three-point bend tests were conducted on a standard tensile test machine using a custom-designed fixture (Figure 4), following the ASTM D2344-84 procedures. The span length between the support rollers was 10 mm, which is approximately four times the specimen thickness. During testing, load was applied through the upper loading roller by downward motion of the crosshead of the tensile machine. A crosshead travel speed of 0.017 mm/s (1 mm/min) was used. A load cell, which was attached to the loading roller, was used to record the loading history.

RESULTS AND DISCUSSION

Microstructural Analysis

Figure 5 shows a typical microstructure of ultrasonically embedded SiC fiber between Al 3003 foils [9]. As can be seen, there were no physical gaps around the fiber, indicating a

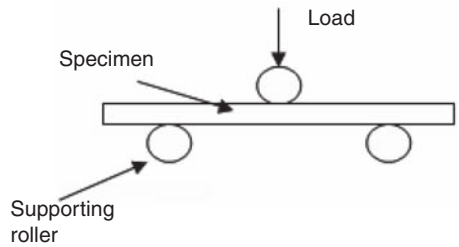

Figure 4. *Setup for three-point bend tests.*

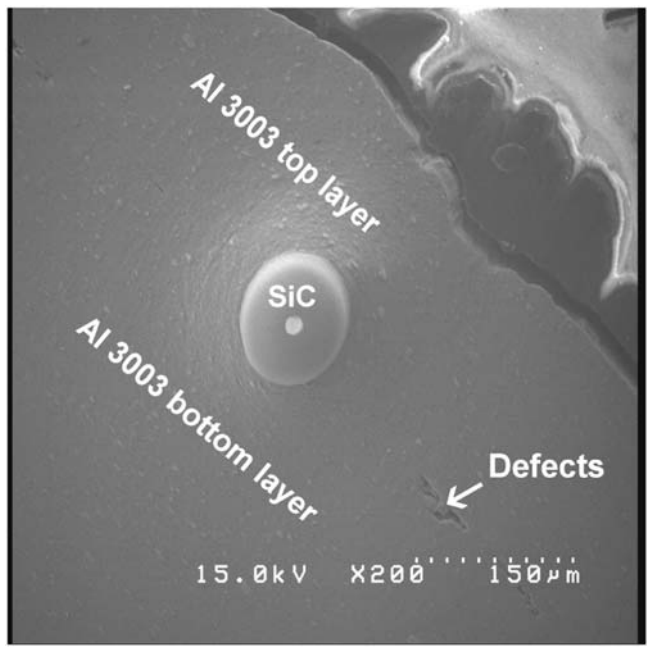

Figure 5. *SEM picture of an embedded SiC fiber between Al 3003 foils [9].*

sound fiber embedment. The cavity between the metal foils introduced by placing a SiC fiber between them was fully filled by the matrix materials, which indicates that the matrix materials in the vicinity of the embedded fiber experienced significant plastic deformation during UC. In a recent study dealing with ultrasonic embedment of SiC fiber in Al 3003 matrices, Li and Soar [10] noticed severely deformed grains and subgrains in the matrix material close to the embedded fibers. The enhanced plastic deformation of the matrix material due to the presence of SiC fibers also facilities good bond formation between the metal foils, even with process parameters which do not promise such good bonding [9]. The mechanical properties of UC-fabricated MMC parts depend on foil–foil and foil–fiber bonding. Good bonding provides effective load transfer from the relatively weak matrix material to the stronger reinforcements (i.e., the embedded SiC fibers), and consequently improves the strength of the parts.

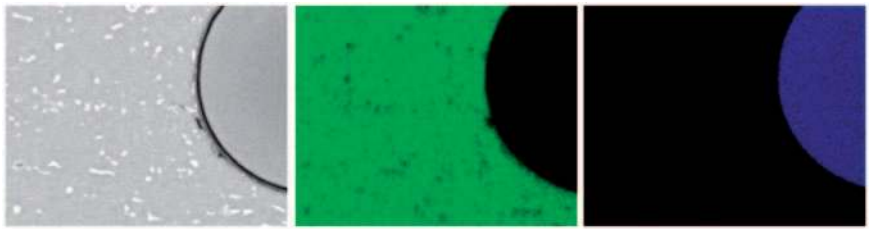

Figure 6. *SEM–EDS area maps.*

Energy dispersive spectroscopy (EDS) studies were carried out on the composite specimens (Figure 6). As can be seen, there was no evidence of significant elemental diffusion across the fiber–matrix interface. Similar findings were reported in an earlier study by Kong [7], in which SiC fibers were embedded between aluminum foils (100 μm thick) using an ultrasonic seam welder equipped with a 50 mm diameter sonotrode.

Peel Tests

In peel tests, the load at which the top foil begins to peel off, termed 'peeling load,' can be taken as a measure of the foil–foil bond strength. The results of peel tests are listed in Table 1. The same are graphically shown in Figure 7 as well. As can be seen in Figure 7, the mean peeling load of Type II specimens was higher than that of Type I specimens, indicating enhanced foil–foil bonding due to the presence of SiC fibers. Since the peel test data showed a high degree of scatter, a hypothesis test for the difference in the means of the peeling loads for the two types of specimens (two-sample t-test) was conducted. The results of this t-test are given in Table 2. The p-value was 0.022, which was smaller than the chosen α-level of 5%. This confirms that the peeling loads of Type I specimens are statistically lower than the peeling loads of Type II specimens at a confidence level of 95%.

An SEM picture of a peeled metal foil from a Type II specimen is shown in Figure 8. As marked on the picture, four distinct zones with different surface features were noticed on the peeled foil. Zone I was an area relatively far from the embedded fiber. The presence of fiber did not seem to significantly influence the foil–foil bond formation in this zone. Thus, the foil–foil bonds formed in Zone I of Type II specimens were the same as the bonds created between the metal foils in Type I specimens. Two kinds of surface topologies were observed in Zone I, a rough surface and a smooth surface (Figure 8(a)). The rough surfaces correspond to the areas where bonds were formed during UC and destroyed during the peel test. A picture of this rough area at higher magnification is shown in Figure 8(b), in which ductile fracture features are evident. The smooth surfaces in Zone I were the areas where the metal foils did not bond during UC. Since, as mentioned previously, the process parameters used for the fabrication of peel test specimens were intended to produce a LWD of 60%, it was expected that about 40% of the overall area away from the fibers would be unbonded after UC.

Zones II and III are areas where the metal foils were well bonded without any unbonded areas or defects. As illustrated in Figure 5, there is a region of enhanced bonding near the fiber, and this region encompasses both Zones II and III. In UC, interfacial foil materials

Table 1. Peeling loads of Type I and Type II specimens.

	Peeling load (N)	
Specimen ID	**Type I**	**Type II**
1	66	58
2	56	58
3	40	54
4	30	62
5	48	79
6	52	94

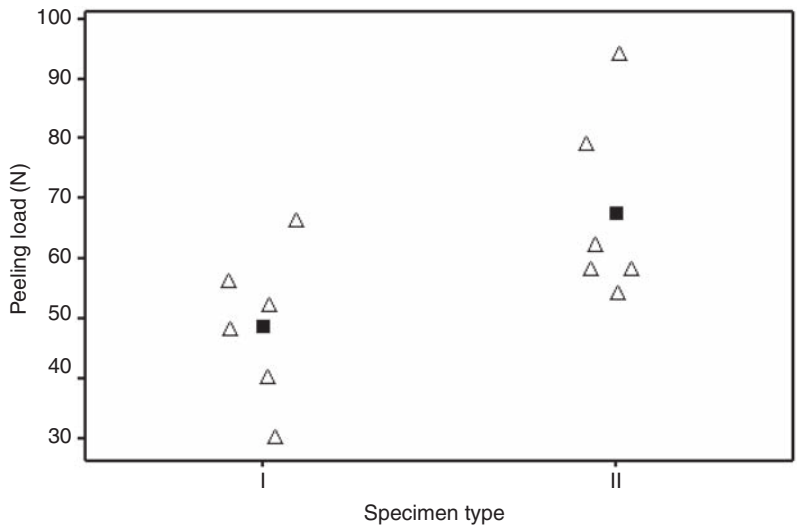

Figure 7. *Results of peel tests (△: result for an individual specimen, ■: mean value for each type of specimen).*

Table 2. Two-sample t-test for peeling loads of two types of specimens.

Type	Number of specimens	Mean	Standard deviation	Standard error of mean
I	6	48.7	12.6	5.1
II	6	67.5	15.7	6.4

t-Test of difference = 0 (vs. <): *t*-value = −2.30, *p*-value = 0.022, and degree of freedom = 10.

experience plastic deformation caused by ultrasonic energy [11,12]. In this case, materials in the vicinity of the fiber (i.e., Zones II and III) experience higher stresses due to combined effects of ultrasonic energy and fiber embedment, than the ones in the regions away from the fiber (i.e., Zone I), which is only affected by ultrasonic energy. As a result, materials undergo enhanced plastic deformation in Zones II and III compared to Zone I. Plastic deformation is an essential condition for producing metallurgical bonding

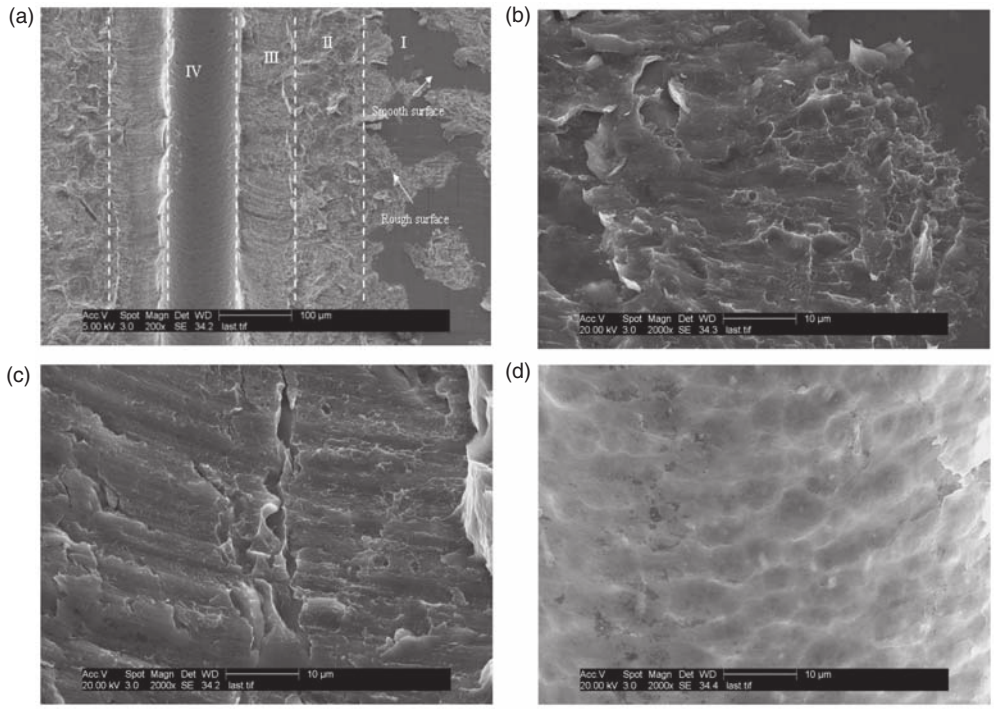

Figure 8. *(a) Failure surface of a peel test specimen, (b) Zone I at high magnification, (c) Zone III at high magnification, and (d) Zone IV at high magnification.*

during UC [11,12]. Plastic deformation facilitates closure of microvoids, which are created by putting two metal surfaces with a certain surface roughness together. Thus, the enhanced plastic deformation near the fiber produces excellent bonding in Zones II and III, which is likely the reason for the improved peeling loads of Type II specimens. In Zone II, ductile fracture features were observed (as in the case of the rough areas in Zone I, Figure 8(b)). In contrast, Zone III showed brittle fracture features (Figure 8(c)). A likely reason for this is excessive strain hardening in Zone III. As stated earlier, in the vicinity of an embedded fiber, the matrix material experiences higher stresses and, consequently, more severe plastic deformation. The stress concentration caused by the fiber decreases as a function of distance away from the fiber. Therefore, the matrix material in Zone III experiences larger plastic deformation and, consequently, higher work hardening than in Zone II, resulting in brittle fracture during the peel test. This is further supported by the work of Li and Soar [10], in which, using nanoindentation hardness tests, the matrix material immediately next to the embedded fiber was shown to have considerably higher hardness than the one in the regions away from the fiber. Another factor which might contribute to brittle fracture near the fiber may be a buildup of oxide fragments in the vicinity of the fiber, which is an area for future research [13].

Zone IV, as shown in Figure 8, corresponds to the groove created on the metal foil by the embedded fiber. The width of this groove was identical to the diameter of the embedded fiber. A higher magnification SEM picture of Zone IV is shown in Figure 8(d). The features in this zone were identical to the exterior surface features of the embedded SiC

fiber (shown in Figure 12(c)). The transference of the surface pattern from the exterior of the SiC fiber to the interior surface of the groove and the fact that no tearing or other failure features were found in this region confirms that the bonding between the fiber and matrix is mechanical entrapment rather than chemical or metallurgical bonding.

Tensile Tests

Typical tensile stress–strain curves of Type I and Type II specimens are shown in Figure 9. In general, four different phases can be observed during uniaxial tensile test of long-fiber-reinforced MMCs, which are: (1) both matrix and fibers deforming elastically, (2) matrix deforming plastically and fibers deforming elastically, (3) both matrix and fibers deforming plastically, and (4) failure of fibers followed by failure of matrix. In Figure 9, stages 1, 2, and 4 can be clearly seen in the stress–strain curve of Type II specimen. However, since SiC fibers are very brittle, stage 3 is not clearly seen in the figure.

The UTS values of Type I and Type II specimens are shown in Figure 10. Interestingly, both types of specimens showed a higher UTS value than the nominal UTS of Al alloy 3003 foil.

During UC, metal foils experience significant plastic deformation and work hardening [10,11,13], which result in the higher UTS of ultrasonically consolidated parts. Also, the mean UTS of Type II specimens was higher than that of Type I specimens due to the presence of SiC fibers in Type II specimens. This was expected, as the Young's modulus and strength of SiC fibers embedded within Type II specimens are much higher than those of the Al 3003 matrix.

Figure 11(a) shows typical fracture features of Type I specimens. As can be seen, delamination between the metal foils occurred during the tensile test. At higher magnifications,

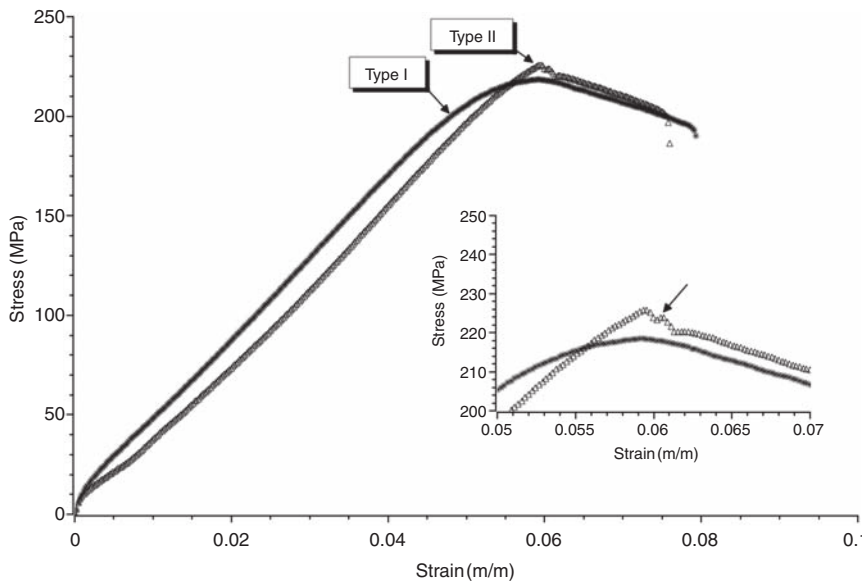

Figure 9. *Tensile stress–strain curves of Type I and Type II specimens. Note: Arrow in the subfigure indicates failure of embedded SiC fibers.*

ductile fracture features were evident in the fractured foils (Figure 11(b)). Figure 12(a) shows the facture surface of a Type II specimen. The embedded SiC fibers between the metal foils can be clearly seen. It is interesting to note that the foil–foil interfaces in the vicinity of embedded fibers did not delaminate during tensile testing, which, once again, evidences stronger foil–foil bonding due to the presence of fibers. On the other hand, as in the case of Type I specimens, regions away from fibers in Type II specimens showed foil–foil delamination (Figure 12(b)). The average UTS of Type I and Type II specimens were 219 and 226 MPa, respectively. While these numbers may not appear significantly different, there is a considerable improvement in the strength, given the low fiber volume fraction used in this study. In fact, the observed improvement is more than what rule of mixtures would predict (222 MPa) (taking the average tensile strength of Type I specimens as the basis). This increase in the tensile strength above the rule of mixtures can be attributed to the enhanced bonding between the layers of the matrix material due to the presence of the fibers.

In Figure 12(c), the exterior surface of an embedded SiC fiber is shown at high magnification. As can be seen, the fiber surface features closely match with the surface features of the groove created on the metal foil in peel tested specimens (Figure 8(d)). Since the hardness of the SiC fiber is much greater than that of the Al matrix, under the application of normal force, the surface pattern of the SiC fiber is imprinted onto the surface of the softer matrix material. This clearly evidences that the fiber is mechanically entrapped between the foils during UC.

Three-point Bend Tests

In three-point bend tests, a factor termed interlaminar shear strength (ISS) was determined for each specimen to evaluate the bond strength between the ultrasonically

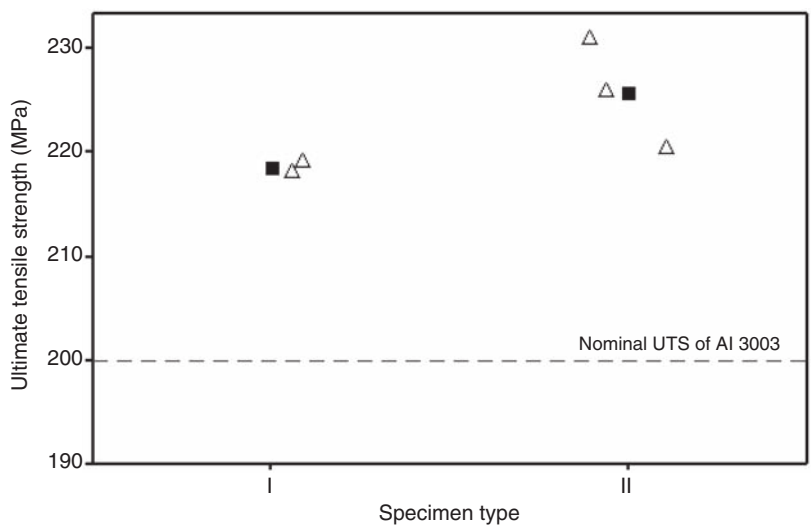

Figure 10. *Results of tensile tests (△: result for an individual specimen, ■: mean value for each type of specimen).*

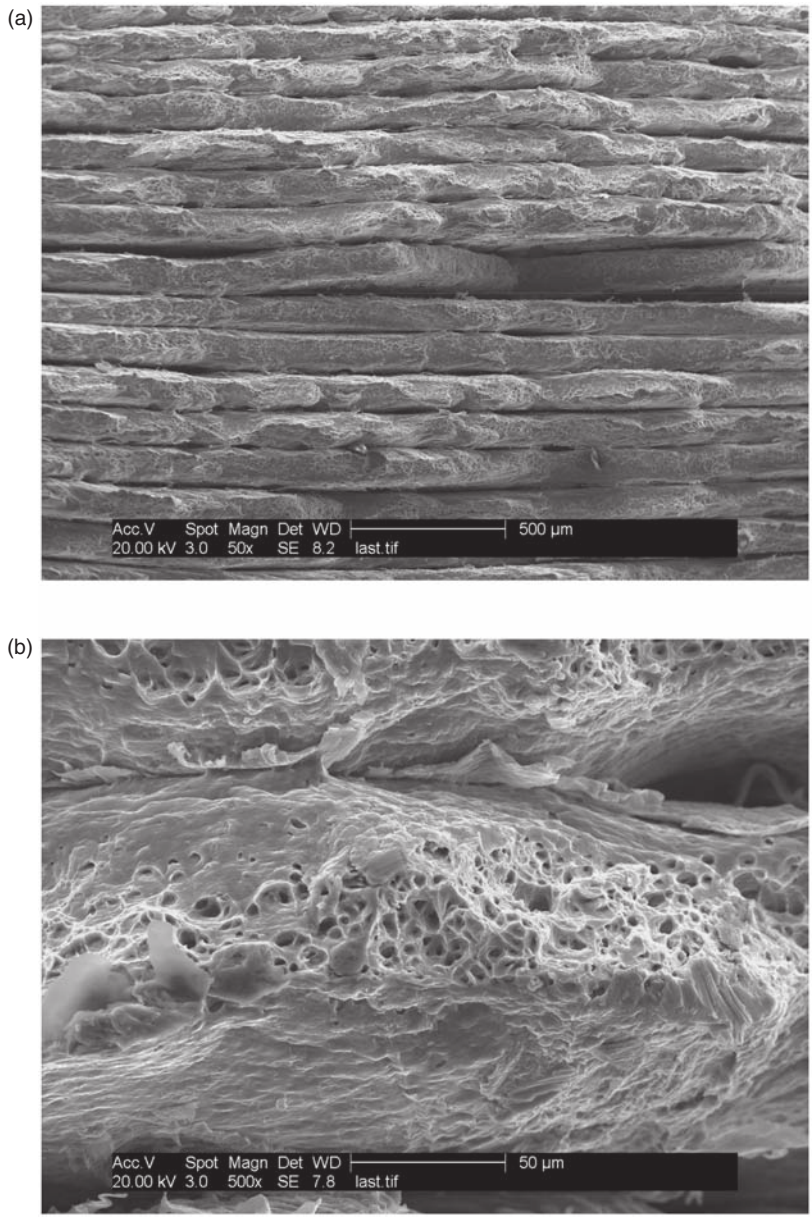

Figure 11. *Tensile fracture surface of a Type I specimen: (a) low magnification and (b) high magnification.*

consolidated metal foils under shear stresses. This factor was computed using the formula described in ASTM standard D2344-84:

$$S_H = \frac{0.75P_{\mathrm{B}}}{bd},$$

where P_{B} was the breaking load (i.e., the maximum load the specimen could bear), b the width of specimen, and d the thickness of the specimen.

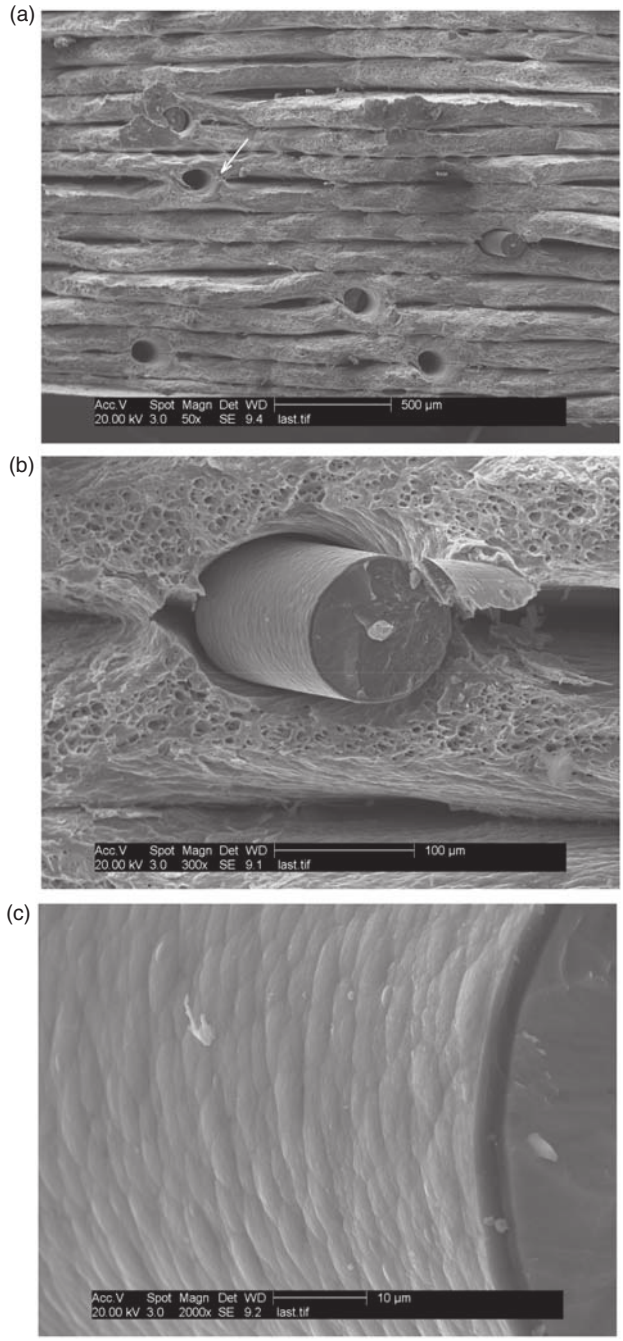

Figure 12. *Tensile fracture surface of a Type II specimen: (a) low magnification (arrow indicates enhanced bonding in the vicinity of the fiber), (b) high magnification, and (c) exterior surface of a SiC fiber at high magnification.*

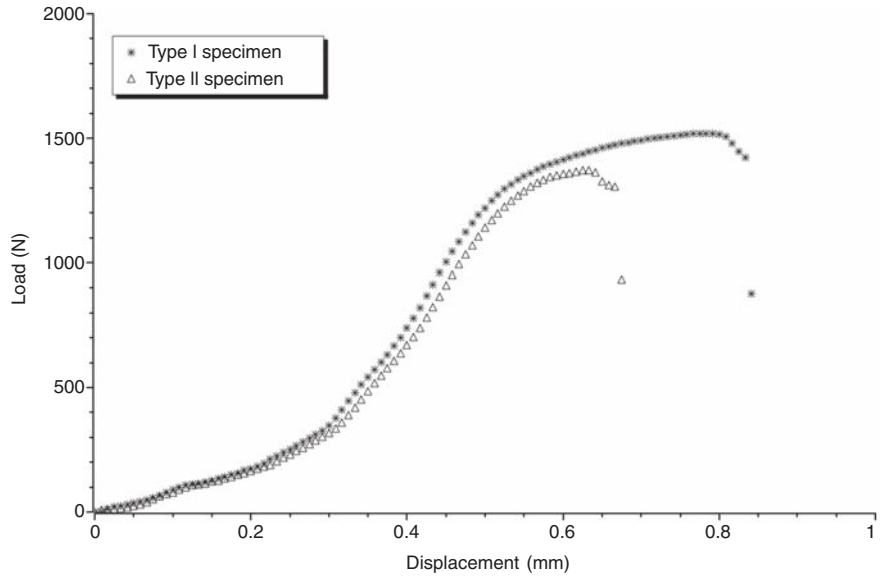

Figure 13. *Load–displacement curves of Type I and Type II specimens obtained in three-point bend tests.*

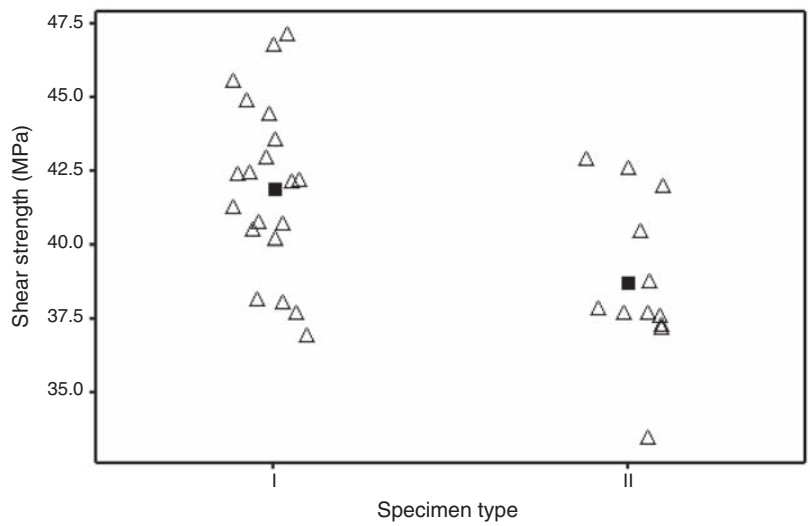

Figure 14. *Results of three-point bend tests (△: results for an individual specimen, ■: mean value for each type of specimen).*

Typical load–displacement curves of Type I and Type II specimens are shown in Figure 13. As can be seen, the shapes of the load–displacement curves of Type I and Type II specimens were very similar. However, Type I specimen withstood considerably higher breaking loads (P_B) than Type II specimens. Figure 14 shows the shear strength values of the two types of specimens. The mean of shear strength of Type II specimens was

Table 3. Two-sample t-test for three-point bend test.

Type	Number of specimens	Mean	Standard deviation	Standard error of mean
I	20	41.92	2.93	0.66
II	12	38.77	2.74	0.79

t-Test of difference = 0 (vs. >): *t*-value = 3.01, *p*-value = 0.003, and degree of freedom = 30.

found to be lower than that of Type I specimens. In view of the scatter in the results, a hypothesis test for the difference in means of ISS for the two types of specimens (two-sample *t*-test) was conducted. The *t*-test results are given in Table 3. The *p*-value for the *t*-test is 0.003, which is smaller than the chosen α-level of 5%. This confirms that the shear strengths of Type I specimens are statistically higher than those of Type II specimens at a confidence level of 95%.

While the ultrasonically embedded SiC fibers served as effective reinforcements under tensile loading conditions along the fiber length, they had some negative effects on the mechanical properties of the parts when subjected to bending loads. It is known that materials respond differently to different loading conditions and show greater susceptibility to certain failure modes. In bend tests, shear stresses of significantly greater magnitude generate at the fiber–matrix interface than in uniaxial tensile testing. Stress concentration effects due to the presence of fibers further amplify the shear stresses at the fiber–matrix interface. Therefore, during bend testing, crack can initiate easily at the fiber–matrix interface as there is nothing at the fiber–matrix interface other than friction due to surface roughness (there is no chemical or metallurgical bonding between the fiber and the matrix to help) to resist the shear stresses.

Based on the findings of this study, UC appears to be a good method of manufacturing fiber-reinforced MMCs. However, due to the mechanical nature of the fiber–matrix bonding achieved in UC, UC-fabricated MMC parts are likely to perform poorly when subjected to bending loads. While further studies are required to confirm this suggestion, future research efforts should focus on devising suitable techniques for improving fiber–matrix bonding in UC MMC parts.

CONCLUSIONS

Peel tests, tensile tests, and three-point bend tests were carried out on UC Al 3003 specimens with and without embedded SiC fibers. In both peel tests and tensile tests, specimens containing SiC fibers showed superior properties compared to those containing no SiC fibers. However, in bend tests, specimens containing no SiC fibers showed better properties than those containing SiC fibers, raising questions about the adequacy of fiber–matrix bonding achieved in UC. Microstructural and fractographic studies provided clear evidence that UC results in mechanical entrapment of fibers, without any chemical interactions between the fiber and the matrix materials.

ACKNOWLEDGMENT

The authors would like to take the opportunity to thank the National Science Foundation (CMMI 0522908) for financially supporting this work.

REFERENCES

1. White, D.R. (2003). Ultrasonic Consolidation of Aluminum Tooling, *Advanced Materials and Processes*, **161**: 64–65.
2. George, J.L. (2006). Utilization of Ultrasonic Consolidation in Fabricating Satellite Decking, Master Thesis, Utah State University, Logan, Utah, USA.
3. Janaki Ram, G.D., Robinson, C.J., Yang, Y. and Stucker, B.E. (2007). Use of Ultrasonic Consolidation for Fabrication of Multi-material Structures, *Rapid Prototyping Journal*, **13**: 226–235.
4. Siggard, E.J. (2007). Investigative Research into the Structural Embedding of Electrical and Mechanical Systems Using Ultrasonic Consolidation, Master Thesis, Utah State University, Logan, Utah, USA.
5. Janaki Ram, G.D., Yang, Y. and Stucker, B.E. (2006). Effect of Process Parameters on Bond Formation During Ultrasonic Consolidation of Aluminum Alloy 3003, *Journal of Manufacturing Systems*, **25**(3): 221–238.
6. Daniels, H.P.C. (1965). Ultrasonic Welding, *Ultrasonics*, **3**: 190–196.
7. Kong, C.Y. (2005). Investigation of Ultrasonic Consolidation for Embedding Active/Passive Fibers in Aluminum Matrices, Doctoral Thesis, Loughborough University, Loughborough, UK.
8. Kong, C.Y. and Soar, R.C. (2005). Fabrication of Metal-Matrix Composites and Adaptive Composites using Ultrasonic Consolidation Process, *Materials Science and Engineering A*, **412**: 12–18.
9. Yang, Y., Janaki Ram, G.D. and Stucker, B.E. (2007). An Experimental Determination of Optimum Processing Parameters for Al/SiC Metal Matrix Composites made using Ultrasonic Consolidation, *Journal of Engineering Materials and Technology*, **129**: 538–549.
10. Li, D. and Soar, R.C. (2008). Plastic Flow and Work Hardening of Al Alloy Matrices during Ultrasonic Consolidation Fiber Embedding Process, *Materials Science and Engineering A*, **498**: 421–429.
11. Yang, Y., Janaki Ram, G.D. and Stucker, B.E. (2009). Bond Formation and Fiber Embedment during Ultrasonic Consolidation, *Journal of Materials Processing Technology*, **209**(10): 4915–4924.
12. Janaki Ram, G.D., Yang, Y., Nylander, C., Aydelotte, B., Stucker, B.E. and Adams, B.L. (2007). Interface Microstructures and Bond Formation in Ultrasonic Consolidation, In: *Proceedings of 18th Solid Freeform Fabrication Symposium*, Austin, TX, USA, August.
13. Zhu, Z., Wynne, B.P. and Ghassemieh, E. (2008). Microstructural Evolution of SiC Fiber Embedded AA6061 Matrix Induced by Ultrasonic Consolidation, In: *MRS Spring Meeting*, San Francisco, CA, 24–28 March, (paper # 1075-J05-03).